

Diverse organic carbon dynamics captured by radiocarbon analysis of distinct compound classes in a grassland soil

Katherine E. Grant^{1*}, Marisa N. Repasch^{1,2,3}, Kari M. Finstad¹, Julia D. Kerr¹, Maxwell Marple¹, Christopher J. Larson^{1,4}, Taylor A. B. Broek^{1,5}, Jennifer Pett-Ridge^{1,5,6}, and Karis J. McFarlane¹

¹Physical and Life Sciences Directorate, Lawrence Livermore National Laboratory, Livermore, CA 94550, USA

²Institute of Arctic and Alpine Research, University of Colorado, Boulder, CO, USA

³Earth and Planetary Sciences, University of New Mexico, Albuquerque, NM, USA

⁴Department of Earth and Environmental Science, University of Pennsylvania, Philadelphia, PA, USA

~~⁵National Ocean Sciences Accelerator Mass Spectrometry (NOSAMS) Facility, Woods Hole Oceanographic Institution Woods Hole, MA, USA~~

⁶Life and Environmental Sciences Department, University of California-Merced, Merced, CA, USA

Correspondence to: Katherine E. Grant (grant39@llnl.gov)

Abstract. Soil organic carbon (SOC) is a large, dynamic reservoir composed of a complex mixture of plant and microbe derived compounds with a wide distribution of cycling timescales and mechanisms. The distinct residence times of individual carbon components within this reservoir depend on a combination of factors, including compound reactivity, mineral association, and climate conditions. To better constrain SOC dynamics, bulk radiocarbon measurements are commonly used to trace biosphere inputs into soils and estimate timescales of SOC cycling. However, understanding the mechanisms driving the persistence of organic compounds in bulk soil requires analyses of SOC pools that can be linked to plant sources and microbial transformation processes. Here, we adapt approaches, previously developed for marine sediments, to isolate organic compound classes from soils for radiocarbon (¹⁴C) analysis. We apply these methods to a soil profile from an annual grassland in Hopland, California (USA) to assess changes in SOC persistence with depth to 1 m. We measured the radiocarbon values of water extractable organic carbon (WEOC), total lipid extracts (TLE), total hydrolysable amino acids (AA), and an acid-insoluble (AI) fraction from bulk and physically separated size fractions (<2 mm, 2 mm–63 μm, and <63 μm). Our results show that Δ¹⁴C values of bulk soil, size fractions, and extracted compound classes became more depleted with depth, and individual SOC components have distinct age-depth distributions that suggest distinguishable cycling rates. We found that AA and TLE cycle faster than the bulk soils and the AI fraction. The AI was the most ¹⁴C depleted fraction, indicating it is the most chemically inert in this soil. Our approach enables the isolation and measurement of SOC fractions that separate functionally distinct SOC pools that can cycle relatively quickly (e.g., plant and microbial residues) from more passive or inert SOC pools (associated with minerals or petrogenic) from bulk soils and soil physical fractions. With the effort to move beyond SOC bulk analysis, we find that compound class ¹⁴C analysis can improve our understanding of SOC cycling and disentangle the physical and chemical factors driving OC cycling rates and persistence.

34 1 Introduction

35 Soil organic carbon (SOC) is a large and complex terrestrial reservoir of Earth's organic carbon (OC) (Jobbágy and
36 Jackson, 2000). It is a highly dynamic and open pool with inputs from decaying plant material, living roots, and soil microbes,
37 and with losses driven by microbial activity that includes the degradation and transformation of compounds (Angst et al.,
38 2021). The result of these processes is a heterogenous mixture of organic compounds with different radiocarbon (^{14}C) ages
39 and reactivities (Lehmann and Kleber, 2015; Shi et al., 2020; Trumbore and Harden, 1997; Gaudinski et al., 2000; McFarlane
40 et al., 2013). This complexity obscures the mechanisms that control overall OC persistence in soils, resulting in a continued
41 debate over the degree to which environmental factors, physical protection, and chemical composition influence SOC reactivity
42 and persistence (Lützow et al., 2006; Lehmann et al., 2020; Schmidt et al., 2011).

43 Bulk analysis methods do not satisfactorily demonstrate how physical protection and chemical composition interact to
44 influence SOC persistence, and so novel organic matter characterization methods can shed light on how different compound
45 classes of OC are preserved in soils and through what mechanisms. For example, we need to understand how the chemical
46 structure of OC influences interactions with mineral surfaces, such as aggregation or sorption, as well as how the environment
47 influences the decomposition and resource availability of certain OC compounds and functional groups (Lehmann and Kleber,
48 2015; Schmidt et al. 2011; Kleber et al., 2021). However, it has been difficult to isolate, identify, and quantify pools of OC
49 ~~that directly link to~~without altering OC molecular chemistry intact or undisturbed~~situ OCOC compounds within the~~
50 ~~soil~~chemical compounds (Von Lutzow et al., 2007). Thus, specific organic compounds isolated from soils, such as amino acids
51 and lipids (Rethemeyer et al., 2004), can provide information on how OC is stabilized in different environments. Therefore,
52 multiple approaches, such as a physical separation followed by a chemical separation, –are needed to fully understand the
53 interplay between chemical compound reactivity and how carbon-mineral interaction functions as part of SOC persistence in
54 soil.

55 One approach used to investigate the controls on SOC persistence is to separate soil into operationally defined carbon
56 pools (e.g., size or density fractions) and characterize the resulting fractions. This approach has demonstrated that association
57 of OC with soil minerals is a critical mechanism for C stabilization (Vogel et al., 2014; Mikutta et al., 2007), as ^{14}C data
58 indicate that some mineral-associated C can persist for thousands of years (Torn et al., 2009). However, ^{13}C labelling
59 experiments show that some mineral-associated C cycles quickly, within months to years (Keiluweit et al., 2015; De Troyer
60 et al., 2011). Some biomolecules form strong associations with mineral surfaces, such as long-chain lipids with iron oxides
61 (Grant et al., 2022), while other compounds only loosely associate with minerals such as through hydrophobic interactions
62 with other OC compounds (Kleber et al., 2007). Therefore, physically isolated mineral-associated OC is still a heterogenous
63 mixture of OC molecules that have a distribution of turnover times, rather than a single homogenous and intrinsically stable
64 SOC pool (Stoner et al., 2023; Van Der Voort et al., 2017).

65 Another approach that can yield finer resolution of OC turnover than traditional techniques is to isolate and measure the

66 isotopic signature of specific compounds (Von Lutzow et al., 2007). In marine, riverine, and lacustrine systems, compound
67 specific radiocarbon analysis (CSRA) has been used monitor the degradation of organic carbon through the marine water
68 column (Loh et al., 2004), characterize marine particulate OC (Hwang and Druffel, 2003), constrain terrestrial OC burial and
69 export from river systems (Galy et al., 2015; Galy et al., 2008; Repasch et al., 2021, Smittenberg et al., 2004), and determine
70 effect of OC export and burial on precipitation patterns and climate (Hein et al., 2020; Eglinton et al., 2021). Different types
71 of compounds including plant or microbial lipid biomarkers (Douglas et al., 2018; Huang et al., 1996), amino acids (Bour et
72 al., 2016; Blattmann et al., 2020), lignin (Feng et al., 2017; Feng et al., 2013), certain carbohydrate compounds (Kuzyakov et
73 al., 2014; Gleixner, 2013), and pyrogenic or black carbon (Coppola et al., 2018) can be isolated and analysed for ^{14}C leading
74 to a more detailed understanding of the cycling of targeted compounds in the environment.

75 Each of these specific compounds can provide information related to the persistence, source, and potential fate of OC in
76 soils. For instance, lipids are found in plant cell walls and microbial cell membranes and are used for energy storage. Amino
77 acids are necessary for protein formation, are enriched in nitrogen relative to other plant and microbial residues, and likely
78 play an important role in nitrogen mining and recycling. These two compound classes have diverse chemical reactivities which
79 allows for insight into chemical compound persistence. Understanding the abundance and age of these two biomarkers in soils
80 can help differentiate the source of C used by soil microbes for metabolism and growth (e.g., new C inputs vs older, recycled
81 soil C) as well as the transformation pathways that yield persistent SOC.

82 Recently, CSRA approaches developed for these environments have been applied to soil showing promise for identifying
83 distinct ages of plant and microbial biomarkers in SOC (Gies et al., 2021; Grant et al., 2022; Van Der Voort et al., 2017; Jia
84 et al., 2023; Douglas et al., 2018). Most of these CSRA studies applied to SOC have targeted specific, individual biomarkers
85 in soils, which generally contribute less than 5% of the entire carbon pool (Lützwow et al., 2006; Kögel-Knabner, 2002). This
86 approach can be too specific to elucidate holistic mechanisms for SOC persistence and turnover that pertain to the majority of
87 SOC. While individual biomarker ages, such as single ages of a particular lipid or single amino acid, can be useful in some
88 contexts, comprehensive understanding of carbon compound class persistence is vital for understanding and modelling the
89 vulnerability of soil carbon to degradation.

90 To strike a balance between too specific and too broad, some researchers have characterized broader compound classes
91 rather than isolating a single biomarker. For example, this ^{14}C -compound class approach has been applied to marine dissolved
92 and particulate OC with a range of compounds, such as total lipids and total amino acids, to provide a broader understanding
93 of OC persistence in oceans (Wang et al., 2006; Wang et al., 1998; [Wang and Druffel, 2001](#); Loh et al., 2004). Wang et al.
94 (1998) established a sequential extraction procedure to analyse ^{14}C abundance of total lipids, amino acids, carbohydrates, and
95 a residual acid insoluble fraction from marine POC and sediments. This approach yielded distinct differences in ^{14}C age and
96 abundance of the amino acids, lipids, and the acid insoluble fraction in POC from the marine water column and sediment, as
97 well as in coastal versus open ocean environments. Loh et al. (2004) found the lipid fraction of dissolved OC and POC to be

98 the oldest fraction measured in both the Atlantic and Pacific oceans, while the acid insoluble fraction was intermediate in age,
99 and the amino acids and carbohydrates contained a significant contribution of modern carbon. Wang and Druffel (2001) also
100 used this approach and found that the lipids were the oldest compound class from sediments in the Southern Ocean, but the
101 acid insoluble residue was very similar in age to the lipid fraction. These studies suggest that compound classes can have
102 independent cycling rates, but these cycling rates can be influenced by the environment.

103 Here, we apply a ^{14}C compound class approach to soils to more broadly understand SOC turnover mechanisms. We
104 characterize the distribution and ^{14}C age of multiple SOC pools with depth in a well-studied annual grassland in California,
105 using soil physical fractionation (McFarlane et al., 2013; Poeplau et al., 2018) and modified compound class extraction
106 methods previously detailed for marine sediments (Wang et al., 1998). We measured the radiocarbon values of water
107 extractable organic carbon (WEOC), total lipid extracts (TLE), total hydrolysable amino acids (AA), and an acid-insoluble
108 (AI) fraction from bulk and physically separated size fractions (bulk soil, sand, and silt+clay). We expected the TLE to be
109 older than its source fraction (bulk soil, sand, or silt+clay), to be older with depth as the decline in plant inputs necessitates
110 recycling and use of older SOC, and to be older in the silt+clay fraction as its high surface area should result in mineral-OC
111 associations that protect SOC from soil microbes- (Grant et al., 2022; Van der vort et al., 2017). We expected the AA to ~~eyele~~
112 ~~faster~~be younger than the TLE fraction and the bulk SOC pool based on the young ^{14}C ages found for AA extracted from in
113 marine sediments (Wang et al., 1998; Wang and Druffel, 2001), but hypothesized that recycling of amino acids at depth by
114 soil microbes might result in an increase in the age of AA below 50 cm. Finally, we expected AI to have old C, similar to the
115 TLE, as seen found in marine sediments (Wang et al., 1998). Here, we describe the relative abundance and radiocarbon content
116 of WEOC, total lipid, ~~and~~ amino acid, and acid insoluble compound class extracts in bulk soils and compare carbon storage
117 and cycling rates within soil size fractions. ~~-~~These data provide a foundation for the continued application of compound class
118 ^{14}C work to the understanding and modelling of soil OC persistence.

119 **2 Materials and Methods**

120 **2.1 Site and Sample Description**

121 Soil samples were collected from the University of California's Hopland Research and Extension Center (HREC) in January
122 2022. The site is an annual grassland with a Mediterranean-type climate, where the mean annual precipitation (MAP) is 940
123 mm per year and mean annual temperature is 15°C (Nuccio et al., 2016). The underlying geology consists of mixed sedimentary
124 rock of the Franciscan formation. The soils are designated Typic Haploxeralfs of the Witherall-Squawrock complex (Soil
125 Survey Staff, 2020). The samples were collected from the "Buck" site (39.001°, -123.069°) where the vegetation is dominated
126 by annual wild oat grass, *Avena barbata* (Kotanen, 2004; Bartolome et al., 2007). Soils were collected from a freshly dug soil
127 pit at four depths: 0–10 cm, 10–20 cm, 20–50 cm, and 50–100 cm. The site is dominated by annual grasses, shallow rooted
128 herbs, and forbs, and we did not observe roots below 10 cm. Thus, root derived inputs of OC are important near the soil surface,

129 but do not directly affect deeper soils at this site. Samples were stored in sealed plastic bags at ambient temperature and
130 transported to the laboratory in Livermore, CA. Soil samples were air dried, homogenized, and sieved to 2 mm, with the >2
131 mm fraction retained for further analysis. Samples were subdivided for soil characterization, physical size separations,
132 chemical compound extractions, and density fractionation.

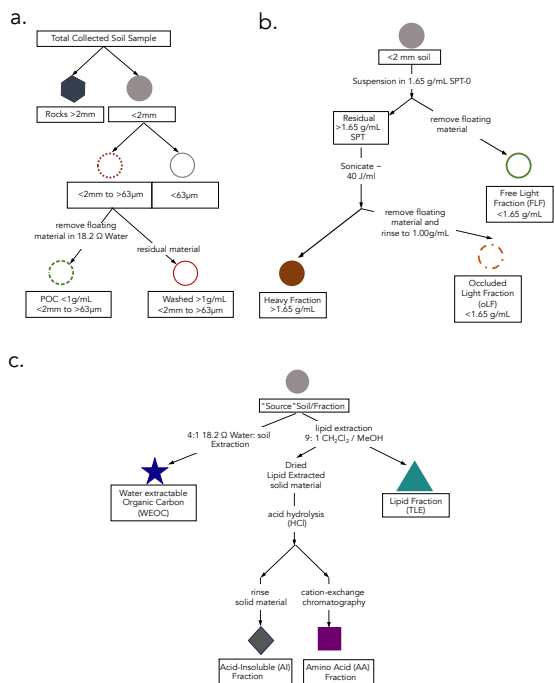
133 **2.2 Physical Fractionation**

134 To compare compound classes between mineral-associated OC and mineral-free OC, we used a salt-free and chemical-free
135 method for isolating the mineral-associated organic matter from the free particulate organic matter (Fig. 1a). Under the
136 assumption that mineral-associated carbon is primarily found in the silt+clay (<63 μm) particle size fraction, we used a size
137 fractionation sieving method where air-dried samples were dry-sieved into three size fractions: bulk soil (<2 mm), sand (2 mm
138 - 63 μm), and silt+clay (<63 μm) (Lavallee et al., 2020; Poeplau et al., 2018). Additionally, because the majority of free
139 particulate organic carbon (POC) is contained in the sand fraction, we used a “water density” separation to remove the low
140 density POC from the mineral matter in this fraction, by suspending the sand fraction in 18.2 M Ω and removing the floating
141 OC, resulting in a POC (<1g mL⁻¹) fraction and a POC-free (>1g mL⁻¹) sand fraction.

142 To further characterize these soils and aid in interpretation of our data, we compared the size fractionated samples to samples
143 separated by density using sodium polytungstate (SPT-0 adjusted to a density of 1.65 g mL⁻¹) (Poeplau et al., 2018) (see SI
144 Section 1.1 for detailed methods). We chose to focus our compound class extraction efforts on size fractionated samples to
145 avoid chemical alteration of SOC during exposure to SPT, since SPT has a high ionic strength and low pH.

146 To constrain any contributions of OC from parent materials to SOC, we processed and analyzed the rock fraction (> 2mm)
147 (Agnelli et al., 2002; Trumbore and Zheng, 1996). Rocks were washed with 18.2 M Ω water in an ultrasonic bath to remove
148 surface contamination, rinsed with 1N HCl to remove any additional weathered material loosely adhered to the surface, dried
149 at 60°C, then manually crushed.

150 A large, representative aliquot (~10 g) of the bulk and each physical fraction were ball milled and measured for total organic
151 carbon (TOC, wt %), C/N ratio, $\delta^{13}\text{C}$ and $\Delta^{14}\text{C}$ (Section 2.6). In addition, we analyzed the bulk soils at each depth with nuclear
152 magnetic resonance (¹³C NMR) to assess the broad structural complexity of the OC in the bulk soil (SI Section 2).



154

155

156

157

158

159

160

161

162

163

164

165

166

167

168

169

170

171

Figure 1: Schematics of protocols used in this study for a) fractionation by size, b.) density separation (details in SI methods), and c) extraction of targeted compound classes. The “sourceparent soil/fraction” refers to the soil from which the different compound classes are extracted. All compound extractions and physical fractionations were applied to the <2 mm bulk soil; total lipid extract (TLE), amino acid (AA), and acid insoluble (AI) compound classes were also extracted from the silt+clay fraction; and only the TLE was extracted from the dense fraction (DF).

2.3 Water-extractable organic carbon (WEOC)

The water-extractable organic carbon (WEOC) fraction was collected from 80 g of bulk soil with 18.2 MΩ water using a 4:1 water to soil ratio (Van Der Voort et al., 2019; Lechleitner et al., 2016; Hagedorn et al., 2004). Saturated soil samples were shaken for 1 hour and then filtered through a pre-rinsed 0.45 µm polyethersulfone (PES) Supor filter under vacuum. An aliquot was taken for dissolved organic carbon (DOC) measurement on a Shimadzu TOC-L combustion catalytic oxidation instrument. Sample concentrations were determined using a nine-point DOC calibration curve ranging from 0–200 mgC L⁻¹. The WEOC fraction was dried using a Labconco CentriVap centrifugal drying system at 40°C and subsequently transferred with 0.1N HCl into pre-combusted quartz tubes to eliminate any inorganic carbon dissolved in the aqueous fraction. The acidified WEOC fractions were then dried down using the CentriVap. Dried samples were flame sealed under vacuum (Section 2.6) for subsequent carbon isotope analyses.

172 **2.4 Total Lipid Extraction (TLE)**

173 Total lipids (TLE) were extracted from the soil samples using an Accelerated Solvent Extraction (ASE) system (Dionex 350,
174 Thermo Scientific) in duplicate. The TLE was extracted from the bulk, sand, silt+clay, and the dense fraction ($> 1.65 \text{ g ml}^{-1}$;
175 DF). An aliquot of 10–30 g of soil was loaded into a stainless-steel ASE extraction cell depending on TOC content (Rethemeyer
176 et al., 2004). The ASE was set to extract the sample for 5 minutes with a holding temperature of 100°C at 1500 PSI. Lipids
177 were extracted using a 9:1 ratio of dichloromethane (DCM or syn: methylene chloride) to methanol (Wang et al., 1998; Van
178 Der Voort et al., 2017; Grant et al., 2022). The TLE was dried under constant ultra-pure N_2 flow at 40°C using a nitrogen dryer
179 (Organomation Multivap Nitrogen Evaporator). The TLE was resuspended in $\sim 5\text{ml}$ of 9:1 DCM:Methanol then transferred to
180 pre-combusted quartz tubes, dried again, and analyzed for ^{14}C as described below (Section 2.5). Total CO_2 produced by the
181 combustion of the TLE was measured manometrically on the ^{14}C vacuum lines during graphitization. Process blank samples
182 were analyzed with each batch (SI Section 3.1).

184 **2.5 Amino Acid (AA) Extraction**

185 Amino acids (AA) were extracted from the lipid-extracted residual bulk and silt+clay size fraction with an acid hydrolysis
186 procedure, desalted, and isolated with cation exchange chromatography using methods modified from those used in marine
187 systems (Wang et al., 1998; Ishikawa et al., 2018; Blattmann et al., 2020). Briefly, a 500 mg soil aliquot was hydrolyzed with
188 6N HCl (ACS grade) under an N_2 atmosphere for 19-24 hours at 110°C . After hydrolysis, amino acids in solution were
189 separated from the solid acid insoluble (AI) fraction via centrifugation for 5 minutes at 2500 rpm. The AI fraction was
190 subsequently washed at a minimum three additional times with 0.2N HCl to ensure complete AA recovery. The supernatant
191 was collected in a single pre-combusted vial and then filtered through a pre-combusted quartz wool fiber plug to remove
192 extraneous sediment particles. The filtered hydrolysate was dried using a CentriVap at 60°C for 4 hours. The dried supernatant
193 was redissolved in 1 ml 0.1N HCl and loaded onto a preconditioned resin column (BioRad 50WX8 200-400 mesh resin) to
194 isolate the AA from other hydrolyzed organic matter and remove excess chloride. Details of the procedure can be found in
195 Ishikawa et al., 2018. Briefly, once the sample was loaded on the column, it was rinsed with three bed volumes ($\sim 6 \text{ ml}$) of 18.2
196 $\text{M}\Omega \text{ H}_2\text{O}$. The free AA were eluted with 10 ml of 2N ammonium hydroxide (NH_4OH), then transferred into pre-baked quartz
197 tubes, dried at 60°C in the CentriVap, and finally sealed and combusted for isotopic analysis. The remaining rinsed solid
198 residual after hydrolysis is the acid-insoluble (AI) fraction. These are processes as a solid sample for isotopic analysis.

200 **2.6 Isotopic and elemental analysis**

201 All samples were analyzed for radiocarbon (^{14}C) at the Center for Accelerator Mass Spectrometry (CAMS) at Lawrence
202 Livermore National Lab (LLNL) in Livermore, California. Samples were either measured on a 10 MV Van de Graaf FN or
203 1MV NEC Compact accelerator mass spectrometer (AMS) (Broek et al., 2021), with average errors of $F^{14}\text{C} = 0.0035$. For

204 solid soil analysis, 10 to 250 mg of ground material was weighed into a pre-combusted quartz tubes along with 200 mg CuO
205 and Ag, flame sealed under vacuum, then combusted at 900°C for 5 hours. The CO₂ was reduced to graphite on preconditioned
206 iron powder under H₂ at 570°C (Vogel et al., 1984). Measured ¹⁴C values were corrected using δ¹³C values and are reported
207 as age-corrected Δ¹⁴C values using the following the conventions of Stuiver and Polach (1977). Extraneous C was quantified
208 for the TLE and AA extractions (SI Table 4 and SI Section 3). For ease of reference, we included conventional radiocarbon
209 ages in our figures and tables. We quantified turnover times using the single pool turnover model described in Sierra et al.
210 (2014) and Van Der Voort et al. (2019) and explained in detail in Trumbore (2000) and Torn et al. (2009). This approach
211 generates two solutions for pools with Δ¹⁴C > 0 ‰, one corresponding to each side of the atmospheric ¹⁴C-CO₂ curve over the
212 last 70 years (Hua et al., 2022). Unfortunately, we cannot identify the correct solution (McFarlane et al., 2013; Trumbore,
213 2000), especially for TLE and AA fractions from the top 20 cm, as we do not have multiple time points or additional constraints
214 such as pool-specific input or decomposition rates (see Section 2.8). Therefore, our data analysis and interpretations rely on
215 the reported Δ¹⁴C values. All individual ¹⁴C measurements used in this study are listed in the Supplementary Information (SI
216 Table 1 and 2).

217 For each solid sample, a dried homogenized aliquot was analyzed for TOC concentration and δ¹³C using an elemental analyzer
218 (CHNOS) coupled to an IsoPrime 100 isotope ratio mass spectrometer at the Center for Stable Isotope Biogeochemistry (CSIB)
219 at the University of California, Berkeley. Samples are assumed to have no inorganic carbon based on acid leaching tests and
220 previously published ¹⁴C work at this site (Finstad et al, 2023, Foley et al., 2023). δ¹³C was measured in duplicate for each
221 solid sample and errors represent the standard deviation of the mean. δ¹³C values of WEOC, TLE, and AA extracts were
222 measured on a split of the cryogenically purified CO₂ and were analyzed at the Stable Isotope Geosciences Facility at Texas
223 A&M University on a Thermo Scientific MAT 253 Dual Inlet Stable Isotope Ratio Mass Spectrometer (SI Table 1).

225 **2.7 Data analysis**

226 Data was analyzed using MATLAB version R20223 and R v. 3.614 (R Core Team, 2019). Linear regressions were calculated
227 between the sample depth mid-point and Δ¹⁴C values from both the size fractions as well as the extracted compounds (WEOC,
228 TLE, AA, AI) from the different size fractions. This was done to directly compare the difference in Δ¹⁴C value between the
229 compound classes. Correlation coefficients, p-values and r² are provided in SI Table 3. Analysis of Variance (ANOVA) was
230 used to assess differences in Δ¹⁴C with depth, between TLE and AA, and between soil fractions. ANOVA tests were performed
231 in R v. 3.614 (R Core Team, 2019). In the text, results are reported as means followed by one standard error when n = 2 or 3
232 or by analytical error when n = 1.

234 **2.8 Interpretation of radiocarbon data**

235 ———In the interpretation of soil ^{14}C activity, we must consider how ^{14}C created during atmospheric nuclear weapons may
236 have affected the isotopic signatures of SOC at our study site. Significantly elevated “bomb” derived ^{14}C was released into the
237 environment during atmospheric nuclear weapons testing during the mid-20th century. This atmospheric radiocarbon spike has
238 been continuously incorporated into carbon reservoirs including vegetation, soils, and oceans (Levin and Hessshaimer, 2000).
239 Plants assimilate CO_2 with the ^{14}C signature of the current year’s atmosphere during photosynthesis and thus incorporate the
240 current atmospheric ^{14}C signature into their tissues and root exudates. This signature then cycles into and through soils as this
241 plant-derived organic matter decays, is processed by microbes, and enters stable soil organic matter pools (Torn et al. 2009).
242 Since the termination of atmospheric weapons testing in the 1960s and with continued fossil fuel emissions, the ^{14}C of
243 atmospheric CO_2 has decreased to approximately pre-1950 values with $0 \pm 1\text{‰}$ reported for the 2019 Northern Hemisphere
244 growing season (Hua et al. 2022). Thus, soil carbon pools with ^{14}C signatures above 0‰ can be interpreted as decadal-aged or
245 decadal cycling C and pools with ^{14}C signatures below 0‰ cycle on century to millennial timescales.

246 **3 Results**

247 **3.1 Radiocarbon values and characterization of the physical fractions**

248 We used soil size and density fractionation to separate the bulk soil into fractions with different degrees of mineral protection.
249 Radiocarbon content for the bulk soil, sand, and silt+clay (SI Table S3) became more ^{14}C depleted (older) with increasing
250 depth (Table 1, Fig. 2). SOC in the silt+clay was consistently younger than in the bulk soil, with the average difference in $\Delta^{14}\text{C}$
251 values increasing from 4‰ at the surface to 87‰ at depth. In the sand fraction, the $\Delta^{14}\text{C}$ values of POC were consistently near
252 current atmospheric values ($2 \pm 3\text{‰}$) and were not significantly correlated with depth. In contrast, the $\Delta^{14}\text{C}$ values of the POC-
253 free sand-sized fraction declined with depth ($25 \pm 3\text{‰}$ to $-510 \pm 2\text{‰}$, $p = 0.006$) and were indistinguishable from the POC-
254 free sand fraction (Fig. 2). Density fractionation of the bulk soil resulted in most of the sample mass ($> 98\%$) and OC (75–
255 83%) recovered in the DF at all depths (SI Fig. S2).

257

258

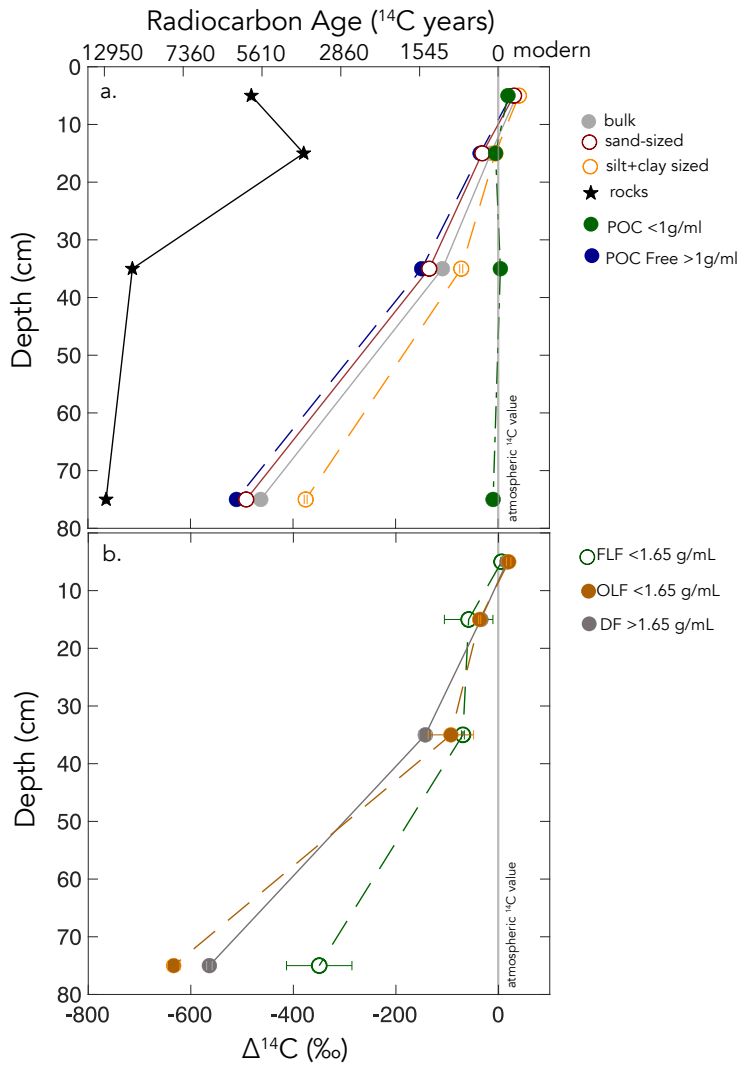
Table 1. Carbon concentrations, mass fractions, and radiocarbon values for the size separations from the Buck Pit

Depth	bulk (<2mm)			sand-sized (2mm to 63 μ m)				silt+clay (<63 μ m)					
	%OC	$\Delta^{14}\text{C} \pm$ err (‰)	<i>mass f</i>	%OC	$\Delta^{14}\text{C} \pm$ err (‰)	POC-free >1g mL ⁻¹		POC <1 g mL ⁻¹			<i>mass f</i>	%OC	$\Delta^{14}\text{C} \pm$ err (‰)
						%OC	$\Delta^{14}\text{C} \pm$ err (‰)	%OC	$\Delta^{14}\text{C} \pm$ err (‰)	<i>mass f</i>			
0-10 cm	3.14	31 \pm 3	0.71	2.68	25 \pm 3	2.08	25 \pm 3	25.69	19 \pm 3	0.29	4.25	34 \pm 3	
10-20 cm	1.22	-22 \pm 3	0.69	0.94	-38 \pm 3	0.77	-35 \pm 3	25.99	-5 \pm 3	0.31	1.84	-13 \pm 3	
20-50 cm	0.50	-116 \pm 3	0.75	0.39	-142 \pm 3	0.38	-149 \pm 2	n.m.	4 \pm 3	0.25	0.85	-79 \pm 3	
50-100 cm	0.25	-468 \pm 3	0.79	0.23	-496 \pm 3	0.18	-510 \pm 2	n.m.	-10 \pm 3	0.21	0.35	-380 \pm 3	

259

260

261



262

263 **Figure 2: $\Delta^{14}\text{C}$ values by depth for a) size-fractions. b) density-fractions from the Buck soil pit. Conventional ^{14}C ages are provided**
264 **for reference. The following abbreviations appear in the legend: particulate organic carbon (POC), free light fraction (FLF),**
265 **occluded light fraction (OLF), and dense fraction (DF).**

266

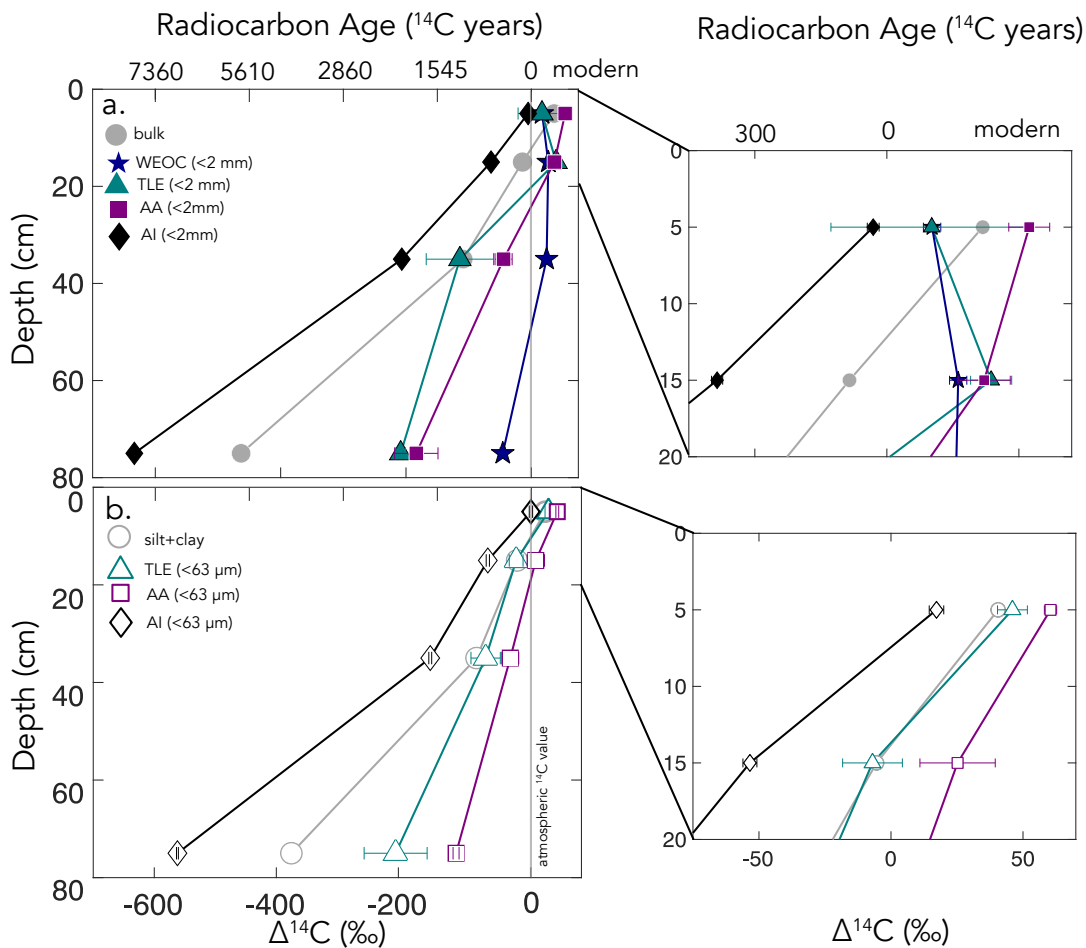
267

268 **3.2 Compound Class results from bulk soil and silt+clay**

269 In both the bulk soil and silt+clay fraction, the extracted compound classes became ^{14}C -depleted with depth except for the
270 WEOC, which had ^{14}C values that reflected C inputs recently fixed from the atmosphere throughout the soil profile (Fig. 2; SI
271 tables). The $\Delta^{14}\text{C}$ values of the WEOC ranged from $14 \pm 4\text{‰}$ at the surface to $-46 \pm 4\text{‰}$ at depth, and the DOC concentrations
272 ranged from 43.2 to $6.7 \text{ mg C g soil}^{-1}$ at the surface and at depth, respectively.

273 The TLE from the bulk soil had $\Delta^{14}\text{C}$ values that range from 17 ± 27 to $-208 \pm 6\text{‰}$ ($n = 2$; \pm SE) in the surface and
274 deepest sample, respectively. In comparison, the TLE from the silt+clay fraction was modern at the surface and became more
275 ^{14}C depleted with depth ($p < 0.001$), from 46 ± 4 to $-204 \pm 36 \text{‰}$. The slopes of the linear regressions of $\Delta^{14}\text{C}$ with depth were
276 indistinguishable in TLE from the bulk soil and silt+clay. In addition, the TLE from the bulk TLE and silt+clay fraction TLE
277 (SI Tables) had very similar $\Delta^{14}\text{C}$ values, but the bulk soil had less lipid-C extracted during each experiment ($280 \text{ } \mu\text{g g C}^{-1}$ in
278 the 0–10 cm vs. $150 \text{ } \mu\text{g g C}^{-1}$; SI Table 2).

279 The $\Delta^{14}\text{C}$ values of the AA extracted from the bulk soil ranged from 54 ± 5 to -183 ± 24 ($n = 2$, SE) with depth (Fig.
280 3, SI Table S3). Similarly, the $\Delta^{14}\text{C}$ value of the AA fraction extracted from silt+clay declined with depth from $60 \pm 3\text{‰}$ ($n =$
281 2 , SE) at the surface to $-106 \pm 4 \text{‰}$ ($n = 2$, SE) at 50–100 cm depth. The slopes of the AA extracted from the bulk and silt+clay-
282 size fractions were statistically different, indicating that the AA extracted from the bulk soil became more depleted with depth
283 than that extracted from the silt+clay (SI Table S3). Furthermore, AA fractions were enriched in ^{14}C relative to the TLE or AI
284 fraction ($p < 0.01$ for bulk soil and $p < 0.05$ for silt+clay). The AI fraction was the oldest fraction found in our study at each
285 depth. The $\Delta^{14}\text{C}$ values of the AI fraction ranged from $-5 \pm 2\text{‰}$ to $-633 \pm 2\text{‰}$ (analytical error, $n=1$) and declined with depth
286 ($p < 0.01$) for bulk soil and silt+clay (Fig. 3; SI Table S3).



287

288 **Figure 3:** a) $\Delta^{14}\text{C}$ by depth for bulk soil and four compound class fractions extracted from bulk soil for the entire depth profile with
 289 the inset of the top 20 cm. b) $\Delta^{14}\text{C}$ by depth for the silt+clay (<63 μm) fraction and three compound classes extracted from the
 290 silt+clay for the entire depth profile with the inset of the top 20 cm. For **total lipid extract (TLE)** and **amino acid (AA)** fractions
 291 ($n=2$) and error bars represent the standard error from duplicate measurements. For the <2 mm, **water extractable organic carbon**
 292 **(WEOC)**, and **acid insoluble (AI)** fractions ($n=1$) and error bars represent analytical error. Error bars are smaller than the marker
 293 width where not shown.

294

295

296 4 Discussion

297 4.1 Variability of ^{14}C in compound classes in soils

298 We measured radiocarbon content of four distinct soil chemical extracts: water extractable organic carbon (WEOC), total
 299 lipid extract (TLE), free amino acids (AA), and the acid insoluble fraction (AI), each of which had distinct $\Delta^{14}\text{C}$ values
 300 compared to the **sourceparent** soil it was extracted from (bulk or silt+clay; Fig. 4a and 4b). The central questions of this study

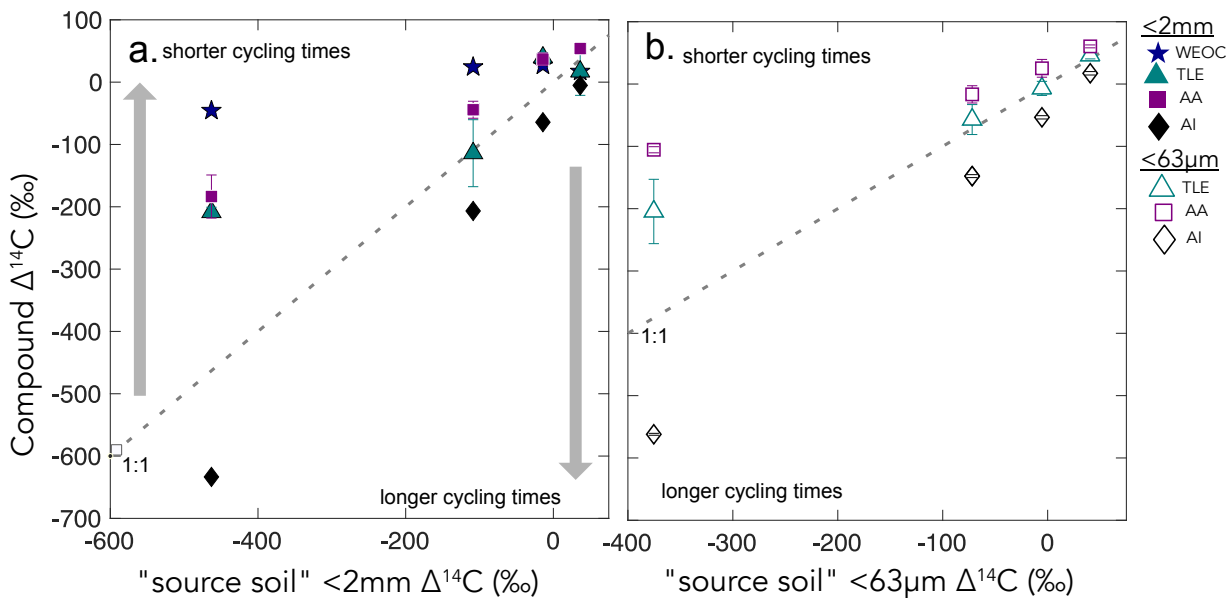
301 are: What are the differences in cycling time/age between various organic compounds in the soil? Do these differences in
302 cycling time change with depth? As expected, $\Delta^{14}\text{C}$ values of TLE, AA, and AI became more depleted with depth (Fig. 2).
303 More interestingly, the differences between the ^{14}C content of parent-source soil and the extracted compounds were not
304 consistent with depth (Fig. 3a and 3b). This divergence in $\Delta^{14}\text{C}$ values reflects differences in turnover times among compound
305 classes, which can be influenced by the sources of OC to each of these pools and by differences in the stabilization mechanisms
306 protecting those compounds from decay. In this annual grassland, plant inputs should have a greater influence on SOC pools
307 near the surface, which we confirmed with near modern $\Delta^{14}\text{C}$ signatures in the 0–10 cm depth for all compound classes and
308 size fractions (Fig. 3b and 3c). Furthermore, at deeper depths, new vegetation inputs should be less readily available, which
309 results in more depleted $\Delta^{14}\text{C}$ signatures at depth and could necessitate microbial use and recycling of older SOC.

310 We found that, averaged across depths, the $\Delta^{14}\text{C}$ values of the TLE were more depleted than those of the AA, though both
311 compound classes were more enriched in $\Delta^{14}\text{C}$ than the bulk soil or silt+clay from which they were extracted. The extracted
312 AAs are the foundational units of hydrolysed proteins and found in both plant and microbial biomass (Blattmann et al., 2020).
313 As in marine studies, we found the AAs to be the youngest compound class fraction (of the TLE and AI) in these soils. The
314 AA pool likely reflects a more actively cycling microbial pool especially at depth, as AA are enriched in nitrogen compounds
315 and likely microbes are both preferentially mining and recycling these compounds (Moe, 2013). The divergence from bulk ^{14}C
316 values indicate that even at depth in the soil, the AAs are either continuously replenished from transport of AAs from surface
317 horizons or re-synthesized with relatively ^{14}C enriched sources such as the WEOC.

318 Based on published data for both soils and marine sediments, we expected the TLE to be older than both the AAs and the
319 bulk soil, however we found that all TLE samples, no matter what fraction we measured, were more ^{14}C enriched than the bulk
320 soil. TLE is composed of a continuum of lipids from plant and microbial materials, ranging from leaf waxes to microbial cell
321 structural components (Angst et al., 2021; Angst et al., 2016), that cycle at different rates and likely interact with mineral
322 surfaces. Previous studies where individual lipid biomarker $\Delta^{14}\text{C}$ values were measured in soils on either short chain or long
323 chain fatty acids found a divergence in $\Delta^{14}\text{C}$ values between these two pools, with short chain lipids generally having enriched
324 ^{14}C values and long chain lipids having more depleted ^{14}C values (Grant et al., 2022; Van Der Voort et al., 2017). For example,
325 long-chain lipid biomarkers, primarily thought to be plant derived, had consistently older ^{14}C ages than bulk soil (Van Der
326 Voort et al., 2017). Short-chain lipids, which can be microbial or root derived (Rethemeyer et al., 2004), were found to be
327 younger than long-chain lipids throughout the soil profiles and younger than bulk soil at depth (Van Der Voort et al., 2017).
328 However, microbial cell wall lipid biomarkers (glycerol dialkyl glycerol tetraethers, GDGTs) had older ^{14}C ages than bulk
329 soils (Gies et al., 2021). With this consideration, our result of more enriched ^{14}C of the TLE could be an indication of a
330 predominance of short chain lipids and suggested higher abundance of microbially-derived lipids than plant-derived lipids.
331 However further study of specific lipid abundance (e.g., *n*-alkanes, fatty acids) in these soils are necessary, as it is unclear to
332 what degree lipids are older than bulk soils with depth because of preservation of these compounds through mineral association

333 or because of microbial use of aged OC sources for growth.

334 We found that AI, the residual sample after both the TLE and AA have been extracted (Wang et al., 1998; Wang et al.,
335 2006). was the most ^{14}C depleted OC fraction measured at each soil depth (Fig. 3, 4) The AI fraction was far more depleted
336 relative to the bulk soil (Fig. 3a and 4a) than observed in marine studies with acid-insoluble OC (Wang et al., 2006; Wang and
337 Druffel, 2001). In these marine studies, the ^{14}C of the AI varied in age depending on sampling depth and location. The
338 significant depletion of the AI in our soils suggests that these chemically stable compounds are not oxidized in soil.
339 Importantly, our AI samples are older than the other chemical and physical soil fractions that we measured in the soil,
340 consistent soil, consistent with the general expectation that aromatic compounds can be difficult to degrade in in soils (Ukalska-
341 Jaruga et al., 2019).



343
344 **Figure 4.** $\Delta^{14}\text{C}$ values of the three extracted compound classes, the water extractable organic carbon (WEOC), the total lipid extract
345 (TLE), the amino acid (AA) fraction, and the acid insoluble (AI) fraction, (y-axis) compared to the $\Delta^{14}\text{C}$ values of the parent or
346 source soil/fraction (x-axis) for a) bulk soil and b) silt+clay. The grey dashed lines show the 1:1 line where bulk sample $\Delta^{14}\text{C}$ equals
347 compound class $\Delta^{14}\text{C}$. Gray arrows point to regions where data plot above or below the 1:1 line, suggesting that a given compound
348 class has shorter and longer carbon turnover times than bulk soil, respectively.
349

350 4.2 Differential OC cycling between the different "parent" fractions fractionation methods

351 Our results suggest different OC cycling timescales for the different physical fractions representing the "sourceparent"
352 fractions. Here, we focus on the silt+clay fraction as an operationally defined mineral-associated OC pool. Numerous soil

353 physical fractionation schemes have been applied to soils and disparities in methods challenge interpretation and
354 intercomparison of results from different studies using different approaches. We compared the size-based soil fractionation to
355 the density fractionation to aid in interpretation and comparability of our findings to other studies. Our silt+clay fraction had
356 higher $\Delta^{14}\text{C}$ values than the sand, POC-free sand, and the dense fraction (DF)~~DF~~. Our silt+clay fraction could include free
357 organic matter that passed through the 63 μm sieve but that would have floated off the DF during density fractionation. For
358 reference, the free light fraction (FLF) has higher $\Delta^{14}\text{C}$ values than the mineral-associated pools and bulk soils (Fig. 5), but
359 also has high C:N reflecting the high OC content and dominantly plant origin of this fraction (SI Table S1). We assume that
360 this small-size free OC is a small fraction of the total silt+clay OC as no small fragments of organic matter were visible and
361 because the C:N ratios of the silt+clay fractions are only slightly elevated compared to the bulk soil and sand fractions (SI
362 Table S1). Rather, the silt+clay fractions may have higher $\Delta^{14}\text{C}$ values relative to the POC-free sand and bulk soil because
363 higher surface area in the silt+clay may facilitate mineral association with surface derived OC ~~with minerals~~ (e.g., from the
364 WEOC fraction).

365 Additionally, our TLE comparison between different size and density fractions highlights the important influence that
366 method selection has over experimental results. Across studies, the mineral-associated OC is not a uniformly defined pool,
367 and the observed results are a consequence of the methodology used to separate the samples (Fig. 6). The mineral-associated
368 TLE cycled more rapidly than the bulk soil no matter which “mineral-associated” fraction (the silt+clay or the dense
369 fraction~~DF~~) was chosen (Fig. 6). The $\Delta^{14}\text{C}$ values of TLE from the bulk, sand, and silt+clay fractions were indistinguishable
370 from one another, possibly because the size fractionation scheme did not effectively separate distinct lipid pools. However,
371 the $\Delta^{14}\text{C}$ values of TLE from the DF were significantly more ^{14}C depleted than TLE from the silt+clay size fraction (Fig. 6),
372 suggesting there were older lipids in the DF relative to the silt+clay. However, more depleted ^{14}C values found in the TLE
373 from the DF compared to the silt+clay could have resulted from the DF being exposed to SPT and/or ground after drying and
374 before lipid extraction. It is possible that grinding the DF prior to lipid extraction increased the exposed surface area and
375 resulted in a larger fraction of old SOC or rock-derived OC being incorporated into the TLE than if the DF had not been
376 ground. ~~Clearly, the approach used to fractionate soils influences experimental results and must be considered when~~
377 ~~interpreting differences in persistence across operationally defined OC pools. We hesitate to definitively choose a best method~~
378 ~~for fractionation because each soil environment and experiment require careful methodological consideration and selection.~~
379 ~~However, given the clear differences in results between MAOM derived from size and density fractionation, it appears grinding~~
380 ~~the samples prior to extraction had significant effects on the age of the resulting TLE. We hesitate to definitively choose a best~~
381 ~~method for fractionation because each soil environment and system make require methodological alteration, however given~~
382 ~~the clear differences in results between the methods. It appears grinding the samples prior to extractions have significant effects~~
383 ~~on the lipid results. Clearly, the approach used to fractionate soils influences experimental results and must be considered~~
384 ~~when interpreting differences in persistence across operationally defined OC pools.~~

385

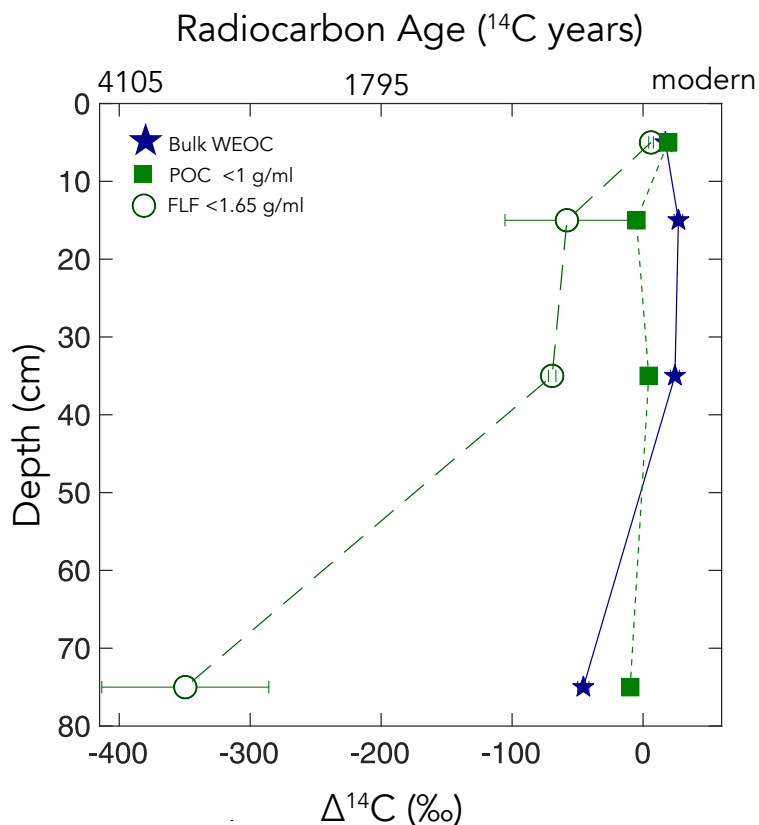
386 4.3 Variation in OC cycling throughout the depth profile

387 The WEOC (extracted from bulk soils) and POC (<1g mL⁻¹ floated off the sand-size fraction) had the highest $\Delta^{14}\text{C}$ values
388 throughout the soil profile, reflecting a predominance of modern carbon from plant detritus and root exudates to these pools.
389 WEOC fractions can comprise a complex mixture of molecules with different structures (Hagedorn et al., 2004; Bahureksa et
390 al., 2021), which are common only in their ability to be mobilized and dissolved in water. WEOC can mobilize and percolate
391 down the soil profile with sufficient precipitation to allow vertical transport. Both the POC and WEOC fractions supply OC
392 that is readily accessible for microbial degradation and microbial utilization – resulting in the rapid turnover and relatively
393 high $\Delta^{14}\text{C}$ values of these two pools (Marin-Spiotta et al., 2011). Occurrence of young OC in deep soils may be driven by
394 microbial uptake of this young and bioavailable DOC or POC. Additionally, we found that the free light-density fractions were
395 depleted in ^{14}C relative to the WEOC and POC (Fig. 5). We suspect this is due to colloidal particles in the FLF, which are not
396 dispersed or dense enough to settle in the SPT.

397 The study site has a Mediterranean climate, and these soils undergo seasonal wetting and drying cycles that may intensify
398 in the future (Swain et al., 2018), potentially shifting the composition or amount of OC that percolates down the soil column,
399 ~~which could shift the age of the OC that the microbial community accesses at depth. When soil is already moist, subsequent~~
400 ~~rainfall may mobilize both OC and colloidal sized mineral material under reducing conditions, which may interact to form~~
401 ~~stable mineral-OC colloids that can enhance the transport of OC down the soil profile and out of the system (Buettner et al.,~~
402 ~~2014). With prolonged dry periods, water soluble OC may be more susceptible to microbial decomposition or oxidation~~
403 ~~because anaerobic preservation is removed (Heckman et al. 2022) This seasonal wetting and drying mechanism likely controls~~
404 ~~what types of organic matter are transported down the soil profile.~~ Deeper in the soil profile, greater reactive mineral surface
405 area and lower microbial activity can enhance carbon stabilization in subsoils (Homyak et al., 2018; Dwivedi et al., 2017; Pries
406 et al., 2023). Further research is needed to understand the effects of seasonal wetting and drying on the behaviour of water-
407 soluble OC in the soil profile.

408 In general, the $\Delta^{14}\text{C}$ values of the TLE, AA, and AI fractions decreased with increasing depth in the profile. While all
409 extracted compounds followed this trend, the degree of ^{14}C depletion with depth varied somewhat between the different
410 compound classes and between the bulk and silt+clay sourceparent fractions. The TLE extracted from the bulk and from the
411 silt+clay fraction had similar slopes with depth. This suggests that depth has more influence than fraction size on resulting
412 lipid ^{14}C content, possibly because of limited transport of lipids down the soil profile. The AAs extracted from the bulk and
413 from the silt+clay fraction differed from one another in that the AA extracted from the bulk soil became more depleted with
414 depth than the AA extracted from the silt+clay. This suggests that at depth, AAs from the silt+clay fraction cycle more quickly
415 than AA's extracted from the bulk soil, possibly indicating that the silt+clay fraction is more directly influenced by microbial
416 activity than the sand fraction. At depths greater than 30 cm, the TLE and AA fraction were markedly younger than the bulk

417 soil, possibly resulting from transport of lipids and amino acids from surface horizons down profile, rapid recycling of these
 418 compounds at depth, the use of a relatively modern C source for lipid and amino acid synthesis at depth, or most likely, a
 419 combination of these. At all depths the AI was significantly older than the sourceparent fraction, indicating that throughout
 420 the soil profile the AI contains an old and stable pool of OC.



421
 422 **Figure 5: Particulate organic carbon (POC) (floated from the sand, n = 1), free light fraction (FLF) (from bulk soil, n = 3, and error**
 423 **bars indicate standard error on the mean), and water extractable organic carbon (WEOC) (from bulk soil, n = 1). $\Delta^{14}\text{C}$ values by**
 424 **depth. For POC and WEOC, error bars indicate analytical error are generally smaller than the symbols.**
 425

426 4.4 Compound class $\Delta^{14}\text{C}$ values in mineral-associated SOC

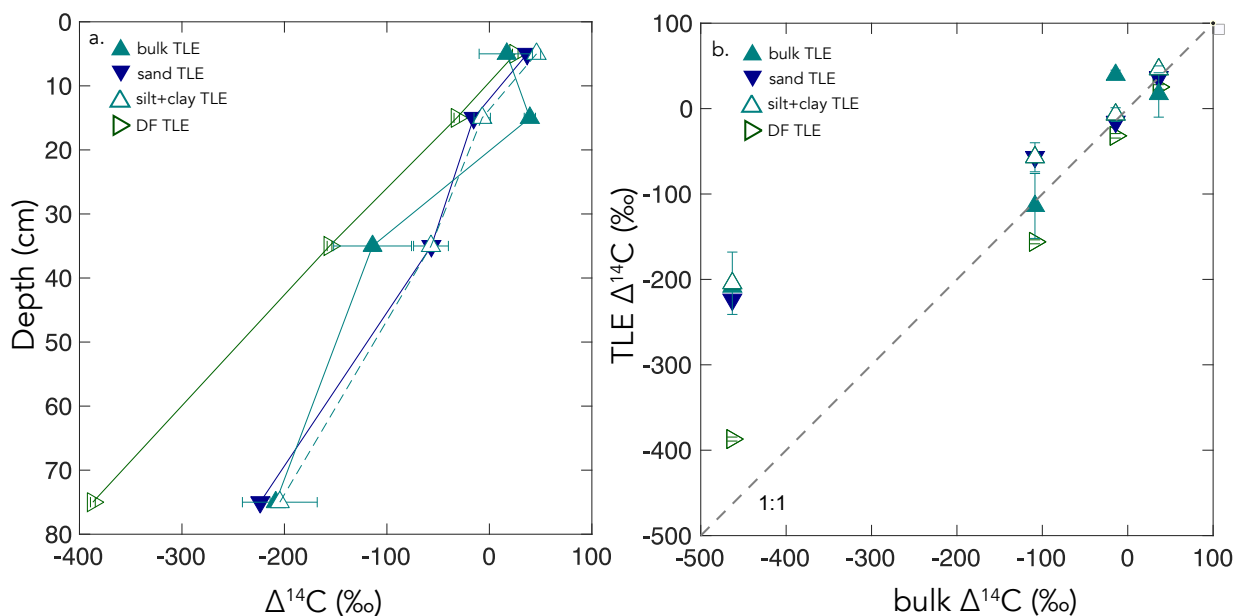
427 To investigate the effect of mineral interaction on the $\Delta^{14}\text{C}$ values or persistence of the TLE, AA, and AI, we measured
 428 these extracted compound classes from physical fractions intended to yield approximate mineral-associated carbon pools. We
 429 focused primarily on the silt+clay size fraction as the physical fraction that best approximates a mineral-associated OC pool
 430 derived from microbially processed plant inputs (Poepflau et al., 2018; Lavalley et al., 2020) and assume that after size
 431 fractionation most of the free organic matter in the bulk soil was in the sand size fraction. We compared the silt+clay size

432 fraction $\Delta^{14}\text{C}$ values to the bulk $\Delta^{14}\text{C}$ values to determine if the material extracted from the isolated mineral-associated fractions
433 of the soil had greater OC persistence or if these compounds cycled indiscriminate of mineral association (Fig. 2).

434 While the TLE from the silt+clay and bulk soil had similar $\Delta^{14}\text{C}$ values, the AA from the silt+clay size fraction was
435 enriched in ^{14}C compared to the AA from bulk soil ($r^2 = 0.98$, $p < 0.05$). This suggests that AAs cycle faster in the silt+clay
436 mineral pool than in the bulk soils. While mineral surfaces usually are thought to promote stability and persistence of OC, in
437 some soil systems, mineral associations may not be the single defining factor of OC persistence (Rocci et al., 2021) and could
438 have a more nuanced role influencing OC cycling in soils.

439 Our data suggests there is a continuum of compounds that exist with different ^{14}C values in the mineral-associated pool,
440 because in the silt+clay fraction, the TLE, AA, and AI have significantly different ^{14}C values (Fig. 4b). For instance, the
441 mineral-associated TLE and AA fractions are enriched in ^{14}C relative to the silt+clay fraction, suggesting both are cycling
442 faster than the average mineral associated pool. However, the AI from the silt+clay fraction is cycling slower than solid sample
443 it was extracted from, and when we compare the AI from the bulk soil to the AI from the silt+clay, the AI from the silt+clay
444 is slightly more ^{14}C enriched. This suggests that there is slight ^{14}C enrichment across compounds in the silt+clay fraction
445 relative to sand and bulk soil.

446 ~~We also compared the TLE extracted from the silt+clay to that extracted from the DF because both fractions are often~~
447 ~~considered mineral associated. Across studies, the mineral associated OC is not a uniformly defined pool, and the observed~~
448 ~~results are a consequence of the methodology used to separate the samples (Fig. 6). The DF TLE $\Delta^{14}\text{C}$ is significantly older~~
449 ~~than the silt+clay TLE (Fig. 6b) and the TLE of the bulk soil at depth (Fig. 6). This Our data suggests that lipids in mineral-~~
450 associated OC pools vary in cycling rates. This is complementary to findings from other studies where ^{14}C values from different
451 lipid biomarkers are divergent from the bulk soils (Gies et al., 2021) and indicates the necessity of looking at entire compound
452 class pools for understanding soil carbon persistence. Further investigation into the composition and age-distribution of
453 compounds within mineral associated-OC is needed to better quantify the distribution of cycling rates within mineral
454 associated OC pools.



455

456 **Figure 6: a) $\Delta^{14}\text{C}$ versus soil depth measured for total lipid extractions (TLE) extractions from four soil size/density fractions, the
 457 bulk (<2mm), sand (63 μm to 2mm), and dense fraction (DF). b) A comparison of the bulk soil $\Delta^{14}\text{C}$ values to the TLE from the four
 458 size/density fractions.**

459

460 4.5 Persistent and Petrogenic OC

461 The most persistent, oldest OC was found in the AI fraction. Because carbon in the AI cycles more slowly than other
 462 components of this grassland soil, it is important to understand what structural components make up the AI and where these
 463 compounds are sourced from. Historically, the chemical structure of the AI fraction has been difficult to characterize. Hwang
 464 and Druffel (2003) argued that the AI is a lipid-like portion of the ocean OC. However, in soils, the AI can be composed of a
 465 mixture of lipid-like compounds and aromatic compounds (Silveira et al., 2008). In our soil, the ^{13}C -NMR spectra of the AI
 466 from 0–10 cm depth show a significant, broad peak in the 100–165 ppm range, indicative of aromatics (SI Fig. 3) (Baldock
 467 and Preston, 1995; Baldock et al., 1997). While it is possible that some condensed aromatic compounds form during the
 468 hydrolysis procedure used to remove AAs, the AI may also contain naturally occurring aromatic compounds that could include
 469 pyrogenic or petrogenic OC.

470 The parent material of our site is a mixture of sandstone, shale, greywacke, and schist (Foley et al., 2022), so it is possible
 471 that some of the OC in our soils is ancient, rock-derived, petrogenic carbon that has been incorporated into the soil profile
 472 through pedogenesis progresses (Grant et al., 2023). Comparison of the AI to the rock (>2 mm) fraction shows that the AI is
 473 younger than the OC contained in the rock fraction (SI Table 1), with the rock fraction $\Delta^{14}\text{C}$ values ranging from -481 to -

765‰. To calculate the contribution of OC_{petro} into the AI fraction, we used a binary mixing model with endmembers of OC_{petro} and aged SOC based on the method in Grant et al. (2023). The $\Delta^{14}\text{C}$ value of the OC_{petro} ^{14}C endmember is -1000 ‰, which is by definition ^{14}C free, -and ~~and~~- the $\Delta^{14}\text{C}$ value of the biospheric endmember was set as either the measured TLE $\Delta^{14}\text{C}$ value or the bulk $\Delta^{14}\text{C}$ value from each depth. This comparison of these two different biospheric endmembers allowed us to calculate a possible range of values for the OC_{petro} contribution (Table 1). In the AI extracted from the silt+clay fraction, the OC_{petro} contribution was 4–5% from 0–10 cm depth and 40–53 % in the 50–100cm depth. In AI extracted from the bulk soil, the OC_{petro} contribution was 0–1 % in the 0–10 cm depth, and 17–44 % in the 50–100 cm depth. Therefore, while the AI fraction likely contains OC_{petro}, it is primarily composed of OC compounds derived from more recent plant and microbial inputs that are highly resistant to acid hydrolysis either because of their chemical structure or their strong associations with minerals.

5 Conclusions and Continued soil radiocarbon compound class characterization

In this study, we characterized a soil carbon profile using compound-class ^{14}C analyses. We found that our extraction methods yielded fractions with ^{14}C signatures distinctly different from the ~~sourceparent~~ soil from which they were extracted. We found that in this annual grassland soil, the AA and the TLE fractions cycle more rapidly than the bulk soil throughout the soil profile. At each depth, the AI fraction is the oldest fraction and contains a combination of slowly cycling SOC and ancient petrogenic C. These results show that soil compound classes cycle differently than similar components in marine systems. Our results also show that mineral-associated SOC contains a mixture of carbon compounds with distinctly different ages and sources that drive turnover and persistence. Compound-specific ^{14}C approaches hold promise for improving our understanding of the chemical structure of SOC, as well as the connection between carbon degradation and preservation in soils. A molecule-resolved understanding of the relationship between compound classes and carbon persistence will also give insight into the fate and turnover time of specific organic biomarkers found in plant residues or the biomass of bacteria, fungi and microfauna. These techniques can also help to determine mechanisms promoting mineral stabilization of soil carbon, especially when combined with soil physical fractionation.

Results from this study highlight that radiocarbon measurements of specific organic compounds and compound classes in soil provide valuable insights into the persistence and decomposition rates of soil organic carbon. To improve our ability to model the future of soil carbon stocks and soil quality in the face of a changing global climate, we need further research that interrogates the composition, radiocarbon content, and cycling rates of soil organic carbon and mechanistically links these rates to physical and chemical drivers.

6 Acknowledgements

This work was performed under the auspices of the U.S. Department of Energy by Lawrence Livermore National Laboratory

506 under Contract DE-AC52-07NA27344 and was supported by the LLNL LDRD Program under Project No. 21-ERD-021 and
507 Project No. 24SI002. LLNL-JRNL-843138. Additional support for site access, sample collection, and site characterization
508 data was provided by the U.S. Department of Energy, Office of Biological and Environmental Research, Genomic Sciences
509 Program LLNL ‘Microbes Persist’ Scientific Focus Area (award #SCW1632). We acknowledge the traditional, ancestral,
510 unceded territory of the Shóqowa and Hopland People, on which this research was conducted. We thank the staff at the Hopland
511 Research and Extension Center who manage the experiment site and Z Kagely for his assistance in digging the soil pit.

512

513 **7 Supplemental Tables/Data Availability**

514 A list of all radiocarbon data, stable carbon, and total OC values with a CAMS tracking number for each of the analyses
515 used in this publication.

516 **8 Author Contributions:** KJM, KMF, TABB, JP, and KEG conceptualized the study. KJM, KMF, TABB, JP secured funding
517 for the project. KEG designed the method and carried out the extractions with input from KJM, KMF, and TABB. CJL carried
518 out the density separations. MNR carried out the water extractions. JDK and MM ran the NMR experiments. KEG, KJM,
519 KMF interpreted the data. KEG prepared the paper with contributions of all co-authors.

520

521 **9 Competing interests.** The authors declare that they have no conflict of interest.

522

523

524 **References**

525

526 Agnelli, A., Trumbore, S. E., Corti, G., and Ugolini, F. C.: The dynamics of organic matter in rock fragments in soil
527 investigated by ¹⁴C dating and measurements of ¹³C, *European Journal of Soil Science*, 53, 147-159,
528 <https://doi.org/10.1046/j.1365-2389.2002.00432.x>, 2002.

529 Angst, G., Mueller, K. E., Nierop, K. G. J., and Simpson, M. J.: Plant- or microbial-derived? A review on the molecular
530 composition of stabilized soil organic matter, *Soil Biology and Biochemistry*, 156, 10.1016/j.soilbio.2021.108189, 2021.

531 Angst, G., John, S., Mueller, C. W., Kögel-Knabner, I., and Rethemeyer, J.: Tracing the sources and spatial distribution of
532 organic carbon in subsoils using a multi-biomarker approach, *Scientific Reports*, 6, 1-12, 2016.

533 Bahureksa, W., Tfaily, M. M., Boiteau, R. M., Young, R. B., Logan, M. N., McKenna, A. M., and Borch, T.: Soil Organic
534 Matter Characterization by Fourier Transform Ion Cyclotron Resonance Mass Spectrometry (FTICR MS): A Critical Review
535 of Sample Preparation, Analysis, and Data Interpretation, *Environmental Science & Technology*, 55, 9637-9656,
536 [10.1021/acs.est.1c01135](https://doi.org/10.1021/acs.est.1c01135), 2021.

- 537 Baldock, J. A. and Preston, C. M.: Chemistry of Carbon Decomposition Processes in Forests as Revealed by Solid-State
538 Carbon-13 Nuclear Magnetic Resonance, in: Carbon Forms and Functions in Forest Soils, 89-117,
539 <https://doi.org/10.2136/1995.carbonforms.c6>, 1995.
- 540 Baldock, J. A., Oades, J. M., Nelson, P. N., Skene, T. M., Golchin, A., and Clarke, P.: Assessing the extent of decomposition
541 of natural organic materials using solid-state ^{13}C NMR spectroscopy, *Soil Research*, 35, 1061-
542 1084, <https://doi.org/10.1071/S97004>, 1997.
- 543 Bartolome, J. W., James Barry, W., Griggs, T., and Hopkinson, P.: 367Valley Grassland, in: *Terrestrial Vegetation of*
544 *California*, edited by: Barbour, M., University of California Press, 0, 10.1525/california/9780520249554.003.0014, 2007.
- 545 Blattmann, T. M., Montluçon, D. B., Haghypour, N., Ishikawa, N. F., and Eglinton, T. I.: Liquid Chromatographic Isolation
546 of Individual Amino Acids Extracted From Sediments for Radiocarbon Analysis, *Frontiers in Marine Science*, 7,
547 10.3389/fmars.2020.00174, 2020.
- 548 Bour, A. L., Walker, B. D., Broek, T. A. B., and McCarthy, M. D.: Radiocarbon Analysis of Individual Amino Acids:
549 Carbon Blank Quantification for a Small-Sample High-Pressure Liquid Chromatography Purification Method, *Analytical*
550 *Chemistry*, 88, 3521-3528, 10.1021/acs.analchem.5b03619, 2016.
- 551 Broek, T. A. B., Ognibene, T. J., McFarlane, K. J., Moreland, K. C., Brown, T. A., and Bench, G.: Conversion of the
552 LLNL/CAMS 1 MV biomedical AMS system to a semi-automated natural abundance ^{14}C spectrometer: system
553 optimization and performance evaluation, *Nuclear Instruments and Methods in Physics Research Section B: Beam*
554 *Interactions with Materials and Atoms*, 499, 124-132, 10.1016/j.nimb.2021.01.022, 2021.
- 555 Buettner, S. W., Kramer, M. G., Chadwick, O. A., and Thompson, A.: Mobilization of colloidal carbon during iron reduction
556 in basaltic soils, *Geoderma*, 221-222, 139-145, <https://doi.org/10.1016/j.geoderma.2014.01.012>, 2014.
- 557 Coppola, A. I., Wiedemeier, D. B., Galy, V., Haghypour, N., Hanke, U. M., Nascimento, G. S., Usman, M., Blattmann, T.
558 M., Reisser, M., Freymond, C. V., Zhao, M., Voss, B., Wacker, L., Schefuß, E., Peucker-Ehrenbrink, B., Abiven, S.,
559 Schmidt, M. W. I., and Eglinton, T. I.: Global-scale evidence for the refractory nature of riverine black carbon, *Nature*
560 *Geoscience*, 11, 584-588, 10.1038/s41561-018-0159-8, 2018.
- 561 De Troyer, I., Amery, F., Van Moorleghe, C., Smolders, E., and Merckx, R.: Tracing the source and fate of dissolved
562 organic matter in soil after incorporation of a ^{13}C labelled residue: A batch incubation study, *Soil Biology and*
563 *Biochemistry*, 43, 513-519, <https://doi.org/10.1016/j.soilbio.2010.11.016>, 2011.
- 564 Douglas, P. M. J., Pagani, M., Eglinton, T. I., Brenner, M., Curtis, J. H., Breckenridge, A., and Johnston, K.: A long-term
565 decrease in the persistence of soil carbon caused by ancient Maya land use, *Nature Geoscience*, 11, 645-649,
566 10.1038/s41561-018-0192-7, 2018.
- 567 Dwivedi, D., Riley, W., Torn, M., Spycher, N., Maggi, F., and Tang, J.: Mineral properties, microbes, transport, and plant-
568 input profiles control vertical distribution and age of soil carbon stocks, *Soil Biology and Biochemistry*, 107, 244-259, 2017.
- 569 Eglinton, T. I., Galy, V. V., Hemingway, J. D., Feng, X., Bao, H., Blattmann, T. M., Dickens, A. F., Gies, H., Giosan, L.,
570 Haghypour, N., Hou, P., Lupker, M., McIntyre, C. P., Montluçon, D. B., Peucker-Ehrenbrink, B., Ponton, C., Schefuss, E.,
571 Schwab, M. S., Voss, B. M., Wacker, L., Wu, Y., and Zhao, M.: Climate control on terrestrial biospheric carbon turnover,
572 *Proc Natl Acad Sci U S A*, 118, 10.1073/pnas.2011585118, 2021.

- 573 Feng, X., Vonk, J. E., Griffin, C., Zimov, N., Montluçon, D. B., Wacker, L., and Eglinton, T. I.: 14C Variation of Dissolved
574 Lignin in Arctic River Systems, *ACS Earth and Space Chemistry*, 1, 334-344, 10.1021/acsearthspacechem.7b00055, 2017.
- 575 Feng, X., Benitez-Nelson, B. C., Montluçon, D. B., Prahl, F. G., McNichol, A. P., Xu, L., Repeta, D. J., and Eglinton, T. I.:
576 14C and 13C characteristics of higher plant biomarkers in Washington margin surface sediments, *Geochimica et*
577 *Cosmochimica Acta*, 105, 14-30, <https://doi.org/10.1016/j.gca.2012.11.034>, 2013.
- 578 Foley, M. M., Blazewicz, S. J., McFarlane, K. J., Greenlon, A., Hayer, M., Kimbrel, J. A., Koch, B. J., Monsaint-Queeney,
579 V., Morrison, K., Morrissey, E., Hungate, B. A., and Pett-Ridge, J.: Active populations and growth of soil microorganisms
580 are framed by mean annual precipitation in three California annual grasslands, *Soil Biology and Biochemistry*, 108886,
581 <https://doi.org/10.1016/j.soilbio.2022.108886>, 2022.
- 582 Galy, V., Peucker-Ehrenbrink, B., and Eglinton, T.: Global carbon export from the terrestrial biosphere controlled by
583 erosion, *Nature*, 521, 204-207, 10.1038/nature14400, 2015.
- 584 Galy, V., Beyssac, O., France-Lanord, C., and Eglinton, T.: Recycling of Graphite During Himalayan Erosion: A Geological
585 Stabilization of Carbon in the Crust, *Science*, 322, 943-945, doi:10.1126/science.1161408, 2008.
- 586 Gaudinski, J. B., Trumbore, S. E., Davidson, E. A., and Zheng, S.: Soil carbon cycling in a temperate forest: radiocarbon-
587 based estimates of residence times, sequestration rates and partitioning of fluxes, *Biogeochemistry*, 51, 33-69,
588 10.1023/A:1006301010014, 2000.
- 589 Gies, H., Hagedorn, F., Lupker, M., Montluçon, D., Haghypour, N., van der Voort, T. S., and Eglinton, T. I.: Millennial-age
590 glycerol dialkyl glycerol tetraethers (GDGTs) in forested mineral soils: 14C-based evidence for stabilization of microbial
591 necromass, *Biogeosciences*, 18, 189-205, 10.5194/bg-18-189-2021, 2021.
- 592 Gleixner, G.: Soil organic matter dynamics: a biological perspective derived from the use of compound-specific isotopes
593 studies, *Ecological Research*, 28, 683-695, 2013.
- 594 Grant, K. E., Hilton, R. G., and Galy, V. V.: Global patterns of radiocarbon depletion in subsoil linked to rock-derived
595 organic carbon, *Geochemical Perspectives Letters*, 25, 36-40, <https://doi.org/10.7185/geochemlet.2312>, 2023.
- 596 Grant, K. E., Galy, V. V., Haghypour, N., Eglinton, T. I., and Derry, L. A.: Persistence of old soil carbon under changing
597 climate: The role of mineral-organic matter interactions, *Chemical Geology*, 587, 10.1016/j.chemgeo.2021.120629, 2022.
- 598 Hagedorn, F., Saurer, M., and Blaser, P.: A 13C tracer study to identify the origin of dissolved organic carbon in forested
599 mineral soils, *European Journal of Soil Science*, 55, 91-100, <https://doi.org/10.1046/j.1365-2389.2003.00578.x>, 2004.
- 600 Hein, C. J., Usman, M., Eglinton, T. I., Haghypour, N., and Galy, V. V.: Millennial-scale hydroclimate control of tropical
601 soil carbon storage, *Nature*, 581, 63-66, 10.1038/s41586-020-2233-9, 2020.
- 602 Homyak, P. M., Blankinship, J. C., Slessarev, E. W., Schaeffer, S. M., Manzoni, S., and Schimel, J. P.: Effects of altered dry
603 season length and plant inputs on soluble soil carbon, *Ecology*, 99, 2348-2362, <https://doi.org/10.1002/ecy.2473>, 2018.
- 604 Hua, Q., Turnbull, J. C., Santos, G. M., Rakowski, A. Z., Ancapichún, S., De Pol-Holz, R., Hammer, S., Lehman, S. J.,
605 Levin, I., Miller, J. B., Palmer, J. G., and Turney, C. S. M.: ATMOSPHERIC RADIOCARBON FOR THE PERIOD 1950–
606 2019, *Radiocarbon*, 64, 723-745, 10.1017/RDC.2021.95, 2022.

- 607 Huang, Y., Bol, R., Harkness, D. D., Ineson, P., and Eglinton, G.: Post-glacial variations in distributions, ^{13}C and ^{14}C
608 contents of aliphatic hydrocarbons and bulk organic matter in three types of British acid upland soils, *Organic Geochemistry*,
609 24, 273-287, [http://dx.doi.org/10.1016/0146-6380\(96\)00039-3](http://dx.doi.org/10.1016/0146-6380(96)00039-3), 1996.
- 610 Hwang, J. and Druffel, E. R. M.: Lipid-Like Material as the Source of the Uncharacterized Organic Carbon in the Ocean?,
611 *Science*, 299, 881-884, doi:10.1126/science.1078508, 2003.
- 612 Ishikawa, N. F., Itahashi, Y., Blattmann, T. M., Takano, Y., Ogawa, N. O., Yamane, M., Yokoyama, Y., Nagata, T., Yoneda,
613 M., Haghypour, N., Eglinton, T. I., and Ohkouchi, N.: Improved Method for Isolation and Purification of Underivatized
614 Amino Acids for Radiocarbon Analysis, *Analytical Chemistry*, 90, 12035-12041, 10.1021/acs.analchem.8b02693, 2018.
- 615 Jia, J., Liu, Z., Haghypour, N., Wacker, L., Zhang, H., Sierra, C. A., Ma, T., Wang, Y., Chen, L., Luo, A., Wang, Z., He, J.-
616 S., Zhao, M., Eglinton, T. I., and Feng, X.: Molecular ^{14}C evidence for contrasting turnover and temperature sensitivity of
617 soil organic matter components, *Ecology Letters*, 26, 778-788, <https://doi.org/10.1111/ele.14204>, 2023.
- 618 Jobbágy, E. G. and Jackson, R. B.: THE VERTICAL DISTRIBUTION OF SOIL ORGANIC CARBON AND ITS
619 RELATION TO CLIMATE AND VEGETATION, *Ecological Applications*, 10, 423-436, [https://doi.org/10.1890/1051-0761\(2000\)010\[0423:TVDOSO\]2.0.CO;2](https://doi.org/10.1890/1051-0761(2000)010[0423:TVDOSO]2.0.CO;2), 2000.
- 621 Keiluweit, M., Bougoure, J. J., Nico, P. S., Pett-Ridge, J., Weber, P. K., and Kleber, M.: Mineral protection of soil carbon
622 counteracted by root exudates, *Nature Climate Change*, 5, 588-595, 2015.
- 623 Kleber, M., Sollins, P., and Sutton, R.: A conceptual model of organo-mineral interactions in soils: self-assembly of organic
624 molecular fragments into zonal structures on mineral surfaces, *Biogeochemistry*, 85, 9-24, 2007.
- 625 Kleber, M. et al., 2021. Dynamic interactions at the mineral–organic matter interface. *Nature Reviews Earth & Environment*,
626 2(6): 402-421.
- 627 Kögel-Knabner, I.: The macromolecular organic composition of plant and microbial residues as inputs to soil organic matter,
628 *Soil Biology and Biochemistry*, 34, 139-162, [https://doi.org/10.1016/S0038-0717\(01\)00158-4](https://doi.org/10.1016/S0038-0717(01)00158-4), 2002.
- 629 Kotanen, P. M.: Revegetation following Soil Disturbance and Invasion in a Californian Meadow: a 10-year History of
630 Recovery, *Biological Invasions*, 6, 245-254, 10.1023/B:BINV.0000022145.03215.4f, 2004.
- 631 Kuzyakov, Y., Bogomolova, I., and Glaser, B.: Biochar stability in soil: Decomposition during eight years and
632 transformation as assessed by compound-specific ^{14}C analysis, *Soil Biology and Biochemistry*, 70, 229-236,
633 <http://dx.doi.org/10.1016/j.soilbio.2013.12.021>, 2014.
- 634 Lavalley, J. M., Soong, J. L., and Cotrufo, M. F.: Conceptualizing soil organic matter into particulate and mineral-associated
635 forms to address global change in the 21st century, *Global Change Biology*, 26, 261-273, <https://doi.org/10.1111/gcb.14859>,
636 2020.
- 637 Lechleitner, F. A., Baldini, J. U. L., Breitenbach, S. F. M., Fohlmeister, J., McIntyre, C., Goswami, B., Jamieson, R. A., van
638 der Voort, T. S., Prufer, K., Marwan, N., Culleton, B. J., Kennett, D. J., Asmerom, Y., Polyak, V., and Eglinton, T. I.:
639 Hydrological and climatological controls on radiocarbon concentrations in a tropical stalagmite, *Geochimica et*
640 *Cosmochimica Acta*, 194, 233-252, <https://doi.org/10.1016/j.gca.2016.08.039>, 2016.
- 641 Lehmann, J. and Kleber, M.: The contentious nature of soil organic matter, *Nature*, 528, 60-68, 10.1038/nature16069, 2015.

- 642 Lehmann, J., Hansel, C. M., Kaiser, C., Kleber, M., Maher, K., Manzoni, S., Nunan, N., Reichstein, M., Schimel, J. P., Torn,
643 M. S., Wieder, W. R., and Kögel-Knabner, I.: Persistence of soil organic carbon caused by functional complexity, *Nature*
644 *Geoscience*, 13, 529-534, 10.1038/s41561-020-0612-3, 2020.
- 645 Levin, I., Heshshaimer, V., 2000. Radiocarbon – A Unique Tracer of Global Carbon Cycle Dynamics. *Radiocarbon*, 42(1):
646 69-80.
- 647 Loh, A. N., Bauer, J. E., and Druffel, E. R. M.: Variable ageing and storage of dissolved organic components in the open
648 ocean, *Nature*, 430, 877-881, 10.1038/nature02780, 2004.
- 649 Lützwow, M. v., Kögel-Knabner, I., Ekschmitt, K., Matzner, E., Guggenberger, G., Marschner, B., and Flessa, H.:
650 Stabilization of organic matter in temperate soils: mechanisms and their relevance under different soil conditions - a review,
651 *European Journal of Soil Science*, 57, 426-445, 10.1111/j.1365-2389.2006.00809.x, 2006.
- 652 Marin-Spiotta, E., Chadwick, O. A., Kramer, M., and Carbone, M. S.: Carbon delivery to deep mineral horizons in Hawaiian
653 rain forest soils, *Journal of Geophysical Research: Biogeosciences*, 116, 2011.
- 654 McFarlane, K. J., Torn, M. S., Hanson, P. J., Porras, R. C., Swanston, C. W., Callahan, M. A., and Guilderson, T. P.:
655 Comparison of soil organic matter dynamics at five temperate deciduous forests with physical fractionation and radiocarbon
656 measurements, *Biogeochemistry*, 112, 457-476, 10.1007/s10533-012-9740-1, 2013.
- 657 Mikutta, R., Mikutta, C., Kalbitz, K., Scheel, T., Kaiser, K., and Jahn, R.: Biodegradation of forest floor organic matter
658 bound to minerals via different binding mechanisms, *Geochimica et Cosmochimica Acta*, 71, 2569-2590, 2007.
- 659 Moe, L. A.: Amino acids in the rhizosphere: From plants to microbes, *American Journal of Botany*, 100, 1692-1705,
660 <https://doi.org/10.3732/ajb.1300033>, 2013.
- 661 Nuccio, E. E., Anderson-Furgeson, J., Estera, K. Y., Pett-Ridge, J., De Valpine, P., Brodie, E. L., and Firestone, M. K.:
662 Climate and edaphic controllers influence rhizosphere community assembly for a wild annual grass, *Ecology*, 97, 1307-
663 1318, 10.1890/15-0882.1, 2016.
- 664 Poeplau, C., Don, A., Six, J., Kaiser, M., Benbi, D., Chenu, C., Cotrufo, M. F., Derrien, D., Gioacchini, P., Grand, S.,
665 Gregorich, E., Griepentrog, M., Gunina, A., Haddix, M., Kuzyakov, Y., Kühnel, A., Macdonald, L. M., Soong, J., Trigalet,
666 S., Vermeire, M.-L., Rovira, P., van Wesemael, B., Wiesmeier, M., Yeasmin, S., Yevdokimov, I., and Nieder, R.: Isolating
667 organic carbon fractions with varying turnover rates in temperate agricultural soils – A comprehensive method comparison,
668 *Soil Biology and Biochemistry*, 125, 10-26, <https://doi.org/10.1016/j.soilbio.2018.06.025>, 2018.
- 669 Pries, C. E. H., Ryals, R., Zhu, B., Min, K., Cooper, A., Goldsmith, S., Pett-Ridge, J., Torn, M., and Berhe, A. A.: The Deep
670 Soil Organic Carbon Response to Global Change, *Annual Review of Ecology, Evolution, and Systematics*, 54, 375-401,
671 10.1146/annurev-ecolsys-102320-085332, 2023.
- 672 R Core Team: R: A language and environment for statistical computing., R Foundation for Statistical Computing [code],
673 2019.
- 674 Repasch, M., Scheingross, J. S., Hovius, N., Lupker, M., Wittmann, H., Haghypour, N., Gröcke, D. R., Orfeo, O., Eglinton,
675 T. I., and Sachse, D.: Fluvial organic carbon cycling regulated by sediment transit time and mineral protection, *Nature*
676 *Geoscience*, 14, 842-848, 10.1038/s41561-021-00845-7, 2021.

- 677 Rethemeyer, J., Kramer, C., Gleixner, G., Wiesenberger, G. L. B., Schwark, L., Andersen, N., Nadeau, M.-J., and Grootes, P.
678 M.: Complexity of Soil Organic Matter: AMS 14C Analysis of Soil Lipid Fractions and Individual Compounds,
679 Radiocarbon, 46, 465-473, 10.1017/S0033822200039771, 2004.
- 680 Rocci, K. S., Lavallee, J. M., Stewart, C. E., and Cotrufo, M. F.: Soil organic carbon response to global environmental
681 change depends on its distribution between mineral-associated and particulate organic matter: A meta-analysis, Science of
682 The Total Environment, 793, 148569, <https://doi.org/10.1016/j.scitotenv.2021.148569>, 2021.
- 683 Schmidt, M. W., Torn, M. S., Abiven, S., Dittmar, T., Guggenberger, G., Janssens, I. A., Kleber, M., Kögel-Knabner, I.,
684 Lehmann, J., and Manning, D. A.: Persistence of soil organic matter as an ecosystem property, Nature, 478, 49-56, 2011.
- 685 Shi, Z., Allison, S. D., He, Y., Levine, P. A., Hoyt, A. M., Beem-Miller, J., Zhu, Q., Wieder, W. R., Trumbore, S., and
686 Randerson, J. T.: The age distribution of global soil carbon inferred from radiocarbon measurements, Nature Geoscience, 13,
687 555-559, 2020.
- 688 Sierra, C. A., Müller, M., and Trumbore, S. E.: Modeling radiocarbon dynamics in soils: SoilR version 1.1, Geoscientific
689 Model Development, 7, 1919-1931, 10.5194/gmd-7-1919-2014, 2014.
- 690 Silveira, M. L., Comerford, N. B., Reddy, K. R., Cooper, W. T., and El-Rifai, H.: Characterization of soil organic carbon
691 pools by acid hydrolysis, Geoderma, 144, 405-414, <https://doi.org/10.1016/j.geoderma.2008.01.002>, 2008.
- 692 Smittenberg, R.H., Eglinton, T.I., Schouten, S., Damsté, J.S.S., 2006. Ongoing Buildup of Refractory Organic Carbon in
693 Boreal Soils During the Holocene. Science, 314(5803): 1283-1286.
- 694 Stoner, S., Trumbore, S. E., González-Pérez, J. A., Schruppf, M., Sierra, C. A., Hoyt, A. M., Chadwick, O., and Doetterl, S.:
695 Relating mineral-organic matter stabilization mechanisms to carbon quality and age distributions using ramped thermal
696 analysis, Philosophical Transactions of the Royal Society A: Mathematical, Physical and Engineering Sciences, 381,
697 20230139, doi:10.1098/rsta.2023.0139, 2023.
- 698 Stuiver, M. and Polach, H. A.: Discussion Reporting of 14C Data, Radiocarbon, 19, 355-363, 10.1017/s0033822200003672,
699 1977.
- 700 Swain, D. L., Langenbrunner, B., Neelin, J. D., and Hall, A.: Increasing precipitation volatility in twenty-first-century
701 California, Nature Climate Change, 8, 427-433, 10.1038/s41558-018-0140-y, 2018.
- 702 Torn, M. S., Swanston, C. W., Castanha, C., and Trumbore, S. E.: Storage and Turnover of Organic Matter in Soil, in:
703 Biophysico-Chemical Processes Involving Natural Nonliving Organic Matter in Environmental Systems, edited by: Senesi,
704 N., Xing, B., and Huang, P. M., Wiley-IUPAC series in biophysico-chemical processes in environmental systems, John Wiley
705 & Sons, Inc., Hoboken, New Jersey, 219-272, 2009.
- 706 Trumbore, S.: Age of Soil Organic Matter and Soil Respiration: Radiocarbon Constraints on Belowground C Dynamics,
707 Ecological Applications - ECOL APPL, 10, 399-411, 10.2307/2641102, 2000.
- 708 Trumbore, S. E. and Harden, J. W.: Accumulation and turnover of carbon in organic and mineral soils of the BOREAS
709 northern study area, Journal of Geophysical Research: Atmospheres, 102, 28817-28830, 10.1029/97jd02231, 1997.
- 710 Trumbore, S. E. and Zheng, S.: Comparison of Fractionation Methods for Soil Organic Matter 14C Analysis, Radiocarbon,
711 38, 219-229, 10.1017/s0033822200017598, 1996.

- 712 Ukalska-Jaruga, A., Smreczak, B., and Klimkowicz-Pawlas, A.: Soil organic matter composition as a factor affecting the
713 accumulation of polycyclic aromatic hydrocarbons, *Journal of Soils and Sediments*, 19, 1890-1900, 10.1007/s11368-018-
714 2214-x, 2019.
- 715 van der Voort, T. S., Mannu, U., Hagedorn, F., McIntyre, C., Walthert, L., Schleppei, P., Haghypour, N., and Eglinton, T. I.:
716 Dynamics of deep soil carbon – insights from 14C time series across a climatic gradient, *Biogeosciences*, 16, 3233-3246,
717 10.5194/bg-16-3233-2019, 2019.
- 718 van der Voort, T. S., Zell, C. I., Hagedorn, F., Feng, X., McIntyre, C. P., Haghypour, N., Graf Pannatier, E., and Eglinton, T.
719 I.: Diverse Soil Carbon Dynamics Expressed at the Molecular Level, *Geophysical Research Letters*, 44, 11,840-811,850,
720 10.1002/2017gl076188, 2017.
- 721 Vogel, C., Mueller, C. W., Höschen, C., Buegger, F., Heister, K., Schulz, S., Schloter, M., and Kögel-Knabner, I.:
722 Submicron structures provide preferential spots for carbon and nitrogen sequestration in soils, *Nature Communications*, 5,
723 2014.
- 724 Vogel, J. S., Southon, J. R., Nelson, D. E., and Brown, T. A.: Performance of catalytically condensed carbon for use in
725 accelerator mass spectrometry, *Nuclear Instruments and Methods in Physics Research Section B: Beam Interactions with*
726 *Materials and Atoms*, 5, 289-293, [https://doi.org/10.1016/0168-583X\(84\)90529-9](https://doi.org/10.1016/0168-583X(84)90529-9), 1984.
- 727 von Lutzow, M., Kogel-Knabner, I., Ekschmitt, K., Flessa, H., Guggenberger, G., Matzner, E., and Marschner, B.: SOM
728 fractionation methods: Relevance to functional pools and to stabilization mechanisms, *Soil Biology and Biochemistry*, 39,
729 2183-2207, 2007.
- 730 Wang, X.-C. and Druffel, E. R. M.: Radiocarbon and stable carbon isotope compositions of organic compound classes in
731 sediments from the NE Pacific and Southern Oceans, *Marine Chemistry*, 73, 65-81, [https://doi.org/10.1016/S0304-](https://doi.org/10.1016/S0304-4203(00)00090-6)
732 [4203\(00\)00090-6](https://doi.org/10.1016/S0304-4203(00)00090-6), 2001.
- 733 Wang, X.-C., Callahan, J., and Chen, R. F.: Variability in radiocarbon ages of biochemical compound classes of high
734 molecular weight dissolved organic matter in estuaries, *Estuarine, Coastal and Shelf Science*, 68, 188-194,
735 10.1016/j.ecss.2006.01.018, 2006.
- 736 Wang, X.-C., Druffel, E. R. M., Griffin, S., Lee, C., and Kashgarian, M.: Radiocarbon studies of organic compound classes
737 in plankton and sediment of the northeastern Pacific Ocean, *Geochimica et Cosmochimica Acta*, 62, 1365-1378,
738 [https://doi.org/10.1016/S0016-7037\(98\)00074-X](https://doi.org/10.1016/S0016-7037(98)00074-X), 1998.
- 739
- 740